

Current Biology, Volume 32

## Supplemental Information

**aPKC regulates apical constriction**

**to prevent tissue rupture**

**in the *Drosophila* follicular epithelium**

**Mariana Osswald, André Barros-Carvalho, Ana M. Carmo, Nicolas Loyer, Patricia C. Gracio, Claudio E. Sunkel, Catarina C.F. Homem, Jens Januschke, and Eurico Morais-de-Sá**

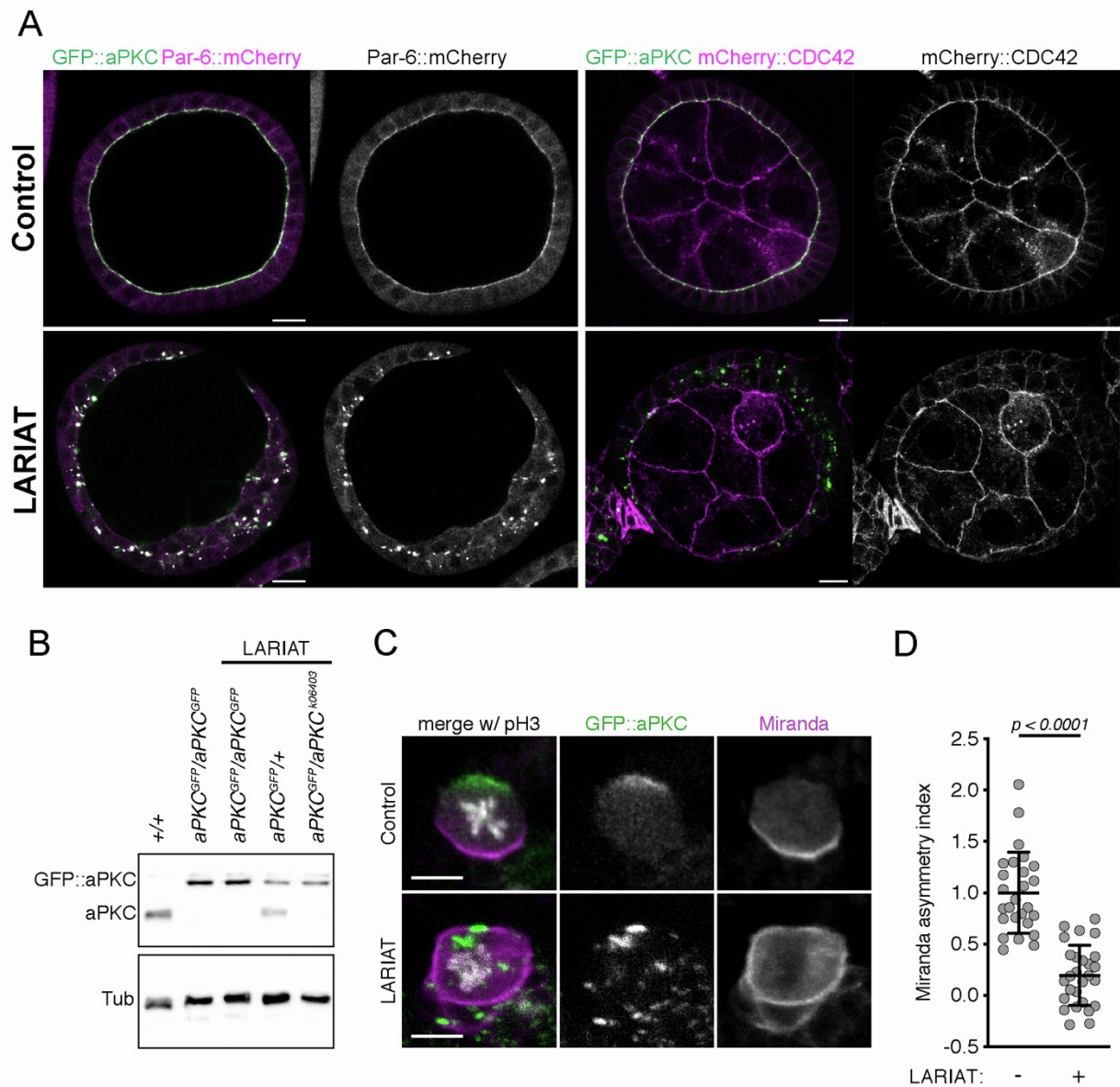


**Figure S1. Optogenetic clustering of GFP::aPKC in *Drosophila* egg chambers and neural stem cells, Related to Figure 1**

**(A)** Par6 is co-sequestered in GFP::aPKC clusters, which do not contain Cdc42. Representative midsagittal images of control and LARIAT egg chambers from flies expressing GFP::aPKC and Par6::mCherry (left) or mCherry::Cdc42 (right) exposed to blue light for 24 hours. Separate channels are shown for Par6 and Cdc42. Scale bars: 10  $\mu$ m **(B)** Western blot shows protein level for untagged and GFP::aPKC in ovaries for the indicated genotypes used in Figure 1C.  $\alpha$ -Tubulin was used as loading control.

**(C,D)** aPKC clustering disrupts Miranda asymmetry in neuroblasts. **(C)** Representative images of control and LARIAT neuroblasts stained for Miranda (magenta) and pH3 to label mitotic cells (grey). Exposure to blue light clustered GFP::aPKC and prevented release of Miranda from the apical cortex. **(D)** Miranda asymmetry index along the cell cortex in control (n = 25 cells) and LARIAT neuroblasts (n = 27 cells) was normalized to control mean value. Graph shows mean  $\pm$  SD values (t-test). Scale bars: 5  $\mu$ m.

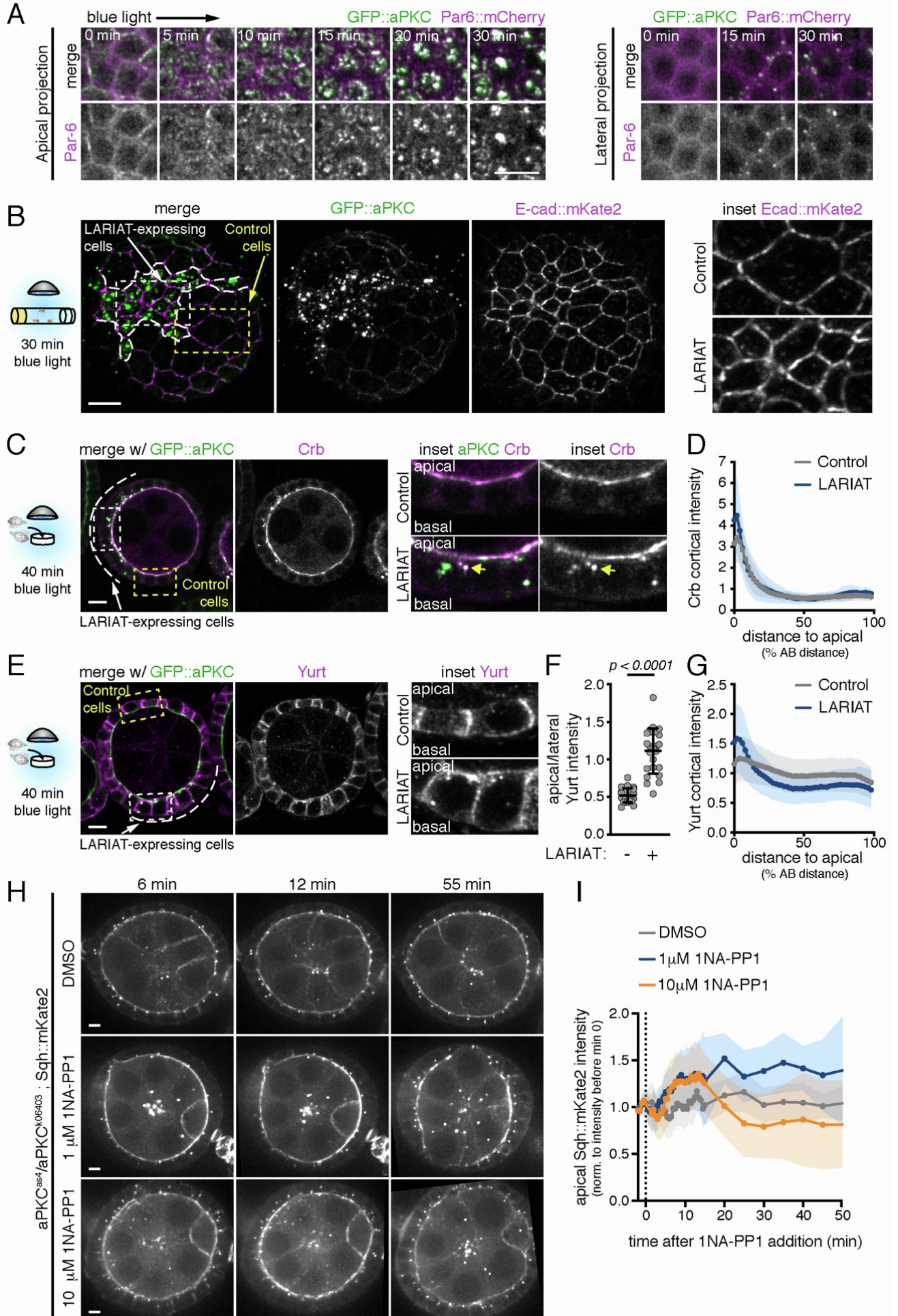




**Figure S2. Acute aPKC inactivation does not disrupt the junctional accumulation of E-cad, but mislocalizes Yurt and upregulates apical myosin, Related to Figure 3.**

**(A)** Par6 co-localizes with aPKC clusters since the beginning of light-exposure. Time-lapse images of egg chambers (surface view) expressing LARIAT, GFP::aPKC and Par6::mCherry. Imaging *ex vivo* with 488 nm laser triggered aPKC clustering from min 0 onwards.

**(B)** Confocal Z-stack projection showing an egg chamber (surface view) that expresses endogenously tagged E-cad::mKate2 and contains mosaic clones of LARIAT cells that cluster GFP::aPKC (green). Exposure of flies to blue light for 30 min reduces the apical area of LARIAT expressing follicle cells but does not disrupt the junctional accumulation of E-cad (magenta). Insets (right) show E-cad::mKate distribution in control and LARIAT cells.

**(C,D)** Crumbs maintains its apical localization even though it partly delocalizes to aPKC clusters. **(C)** Confocal midsagittal image of follicular epithelium that contains mosaic clones of LARIAT expressing cells (white dashed contour) that cluster GFP::aPKC (green) and were stained for Crb (magenta, separated grey channel and inset). Exposure of flies to blue light for 40 min maintains Crb at the apical level with some Crb signal co-localizing at aPKC clusters. **(D)** Distribution of Crb cortical intensity along the apical-basal axis in control (n = 92 cells, 23 egg chambers) and LARIAT (n = 82 cells, 23 egg chambers) clones. Fluorescence intensity normalized to the average intensity of all control cell interfaces in the same egg chamber. Graph show mean  $\pm$  SD.

**(E-G)** Yurt is mislocalized to the apical domain upon optogenetic perturbation of aPKC. **(E)** Confocal midsagittal image of follicular epithelium that contains mosaic clones of UAS-LARIAT expressing cells (white dashed contour) that cluster GFP::aPKC (green) and were stained for Yurt (magenta, separated channel and inset). Exposure to blue light for 40 min increases Yurt intensity at the apical level (arrow). **(F)** Ratio of apical/lateral Yurt mean fluorescence intensity in control (n = 338 cells, 23 egg chambers) and LARIAT (n = 327 cells, 24 egg chambers) clones. Graph show mean  $\pm$  SD, grey points represent average for individual egg chambers. Unpaired t-test was used. **(G)** Distribution of Yurt cortical intensity along the apical-basal axis in control (n = 92 cells, 23 egg chambers) and LARIAT (n = 82 cells, 23 egg chambers) clones. Fluorescence intensity was normalized to the average intensity of all control cell interfaces in the same egg chamber. Graph shows mean  $\pm$  SD.

**(H)** Time-lapse midsagittal images of *aPKC<sup>as4</sup>/aPKC<sup>k06403</sup>* egg chambers expressing Sqh::mKate2. The indicated concentrations of 1NA-PP1 were added at time 0. **(I)** Sqh intensity at the apical surface was corrected for cytoplasm intensity and normalized to average intensity prior to aPKC inhibition (n  $\geq$  32 cells from  $\geq$  2 egg chambers per condition). Scale bars: 5  $\mu$ m.

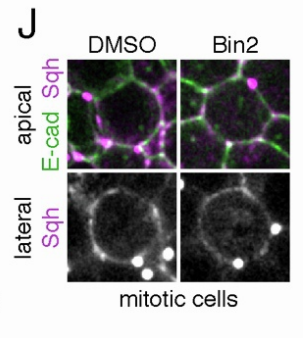
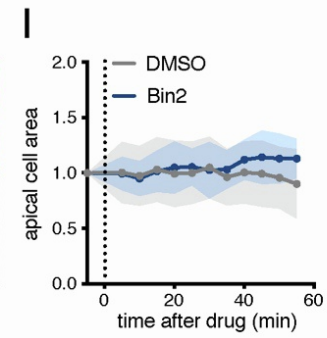
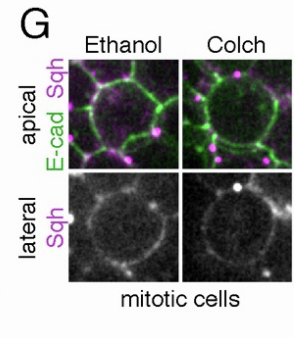
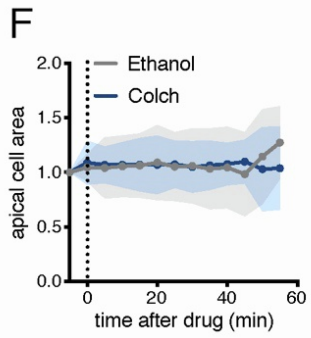
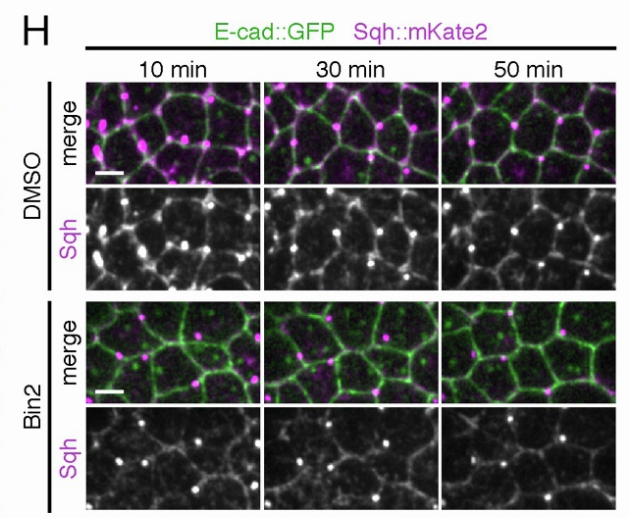
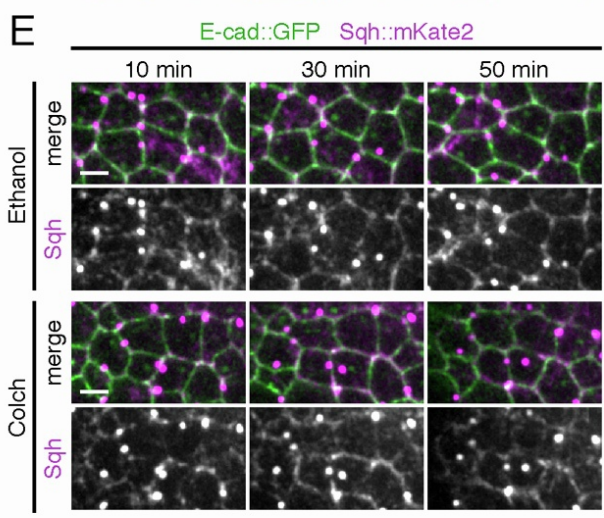
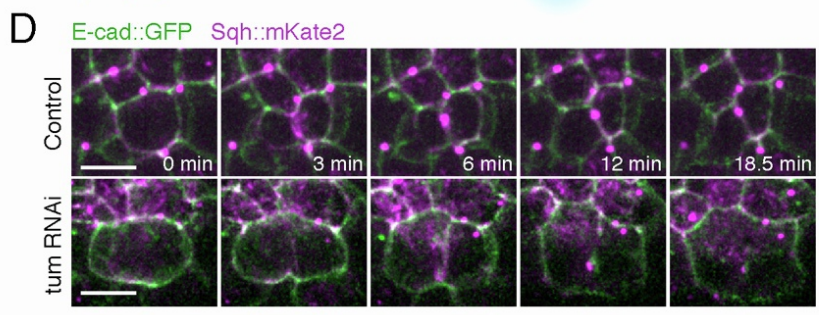
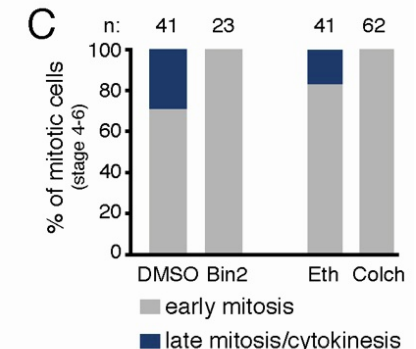
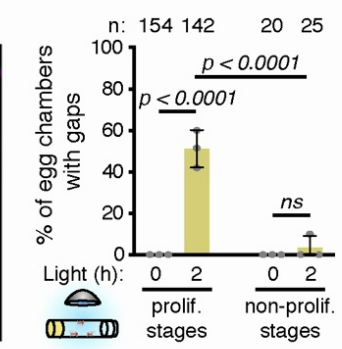
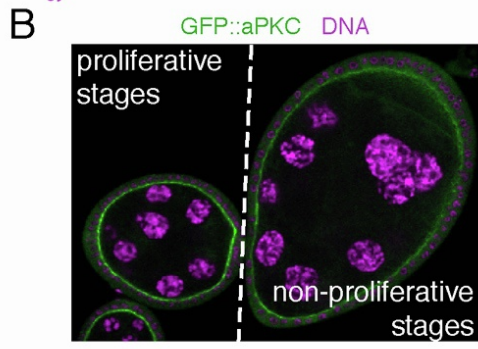
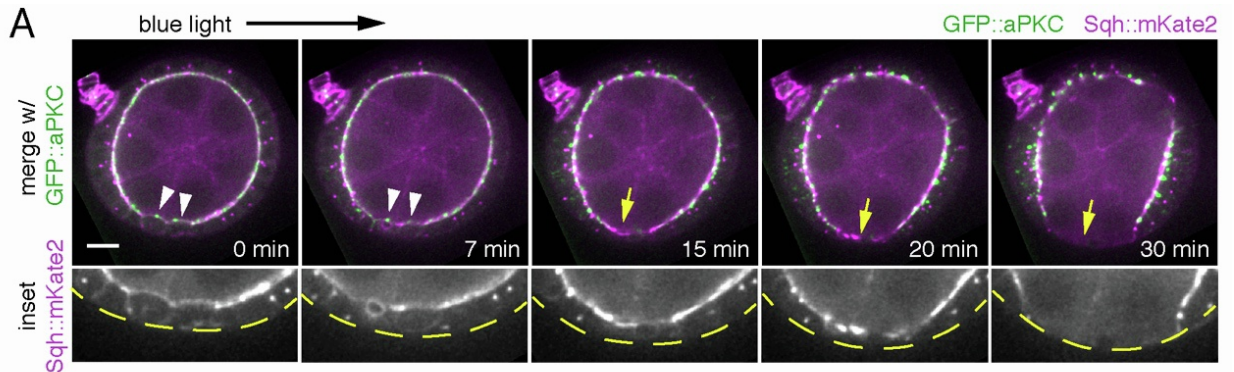


**Figure S3. Formation of epithelial gaps during cell division upon aPKC clustering, Related to Figure 5.**

**(A)** Time-lapse images of egg chambers (midsagittal view) expressing LARIAT, GFP::aPKC (green) and Sqh::mKate2 (magenta). Imaging with 488nm laser clustered aPKC from min 0 onwards. Epithelial gap (yellow arrow) forms where cells divided (white arrowheads); dashed line delineates egg chamber in Sqh inset.

**(B)** Quantification of epithelial gaps in proliferative (stages 4-6) and non-proliferative (analysis restricted to stage 8 egg chambers to ensure the sample was non-proliferative during the 2h of light exposure). GFP::aPKC homozygous egg chambers expressing LARIAT and exposed to light *in vivo* for 0 or 2h before ovary fixation. Graphs show mean  $\pm$  SD (Fisher's test); grey data points represent percentage from independent experiments; n = number of egg chambers scored.

**(C-D)** Validation of the genetic and drug perturbations used to perturb cytokinesis **(C)** Quantification of the frequency of mitotic cells in early *versus* late mitosis (anaphase onwards) in egg chambers treated with Binucleine-2 (Bin2) or Colchicine (Colch) confirms that both drugs disrupt cytokinesis initiation when compared to the respective controls. Mitotic cells were scored in egg chambers stained for phospho-Ser10 on Histone H3, actin and DNA. n = number of mitotic cells scored. **(D)** Live imaging of cell division in follicle cells expressing Sqh::mKate2 and E-cad::GFP in control and Tum RNAi egg chambers. Tum-depleted cells start to constrict but fail cytokinesis (cytokinesis onset at min 0).

**(E-J)** Treatment with Bin2 or Colch on their own does not produce a significant change in apical cell area and allows mitotic rounding during cell division. **(E,H)** Time-lapse images of follicular epithelium (surface views) expressing E-cad::GFP and Sqh::mKate2 in egg chambers treated with (E) Bin2, (H) Colch or respective controls. Time is shown in reference to the moment of drug addition. **(F,I)** Apical surface area (mean  $\pm$  SD) measured at the junction level and normalized to the initial value of each time-lapse movie (Ethanol: n = 17; Colch: n = 19; DMSO: n = 20; Bin2: n = 12). **(G,J)** Close-up of mitotic cells expressing E-cad::GFP and Sqh::mKate2 in egg chambers treated with (G) Bin2, (J) Colch or respective controls.

Scale bars = (A) 10  $\mu$ m (D,E,H) 5  $\mu$ m.



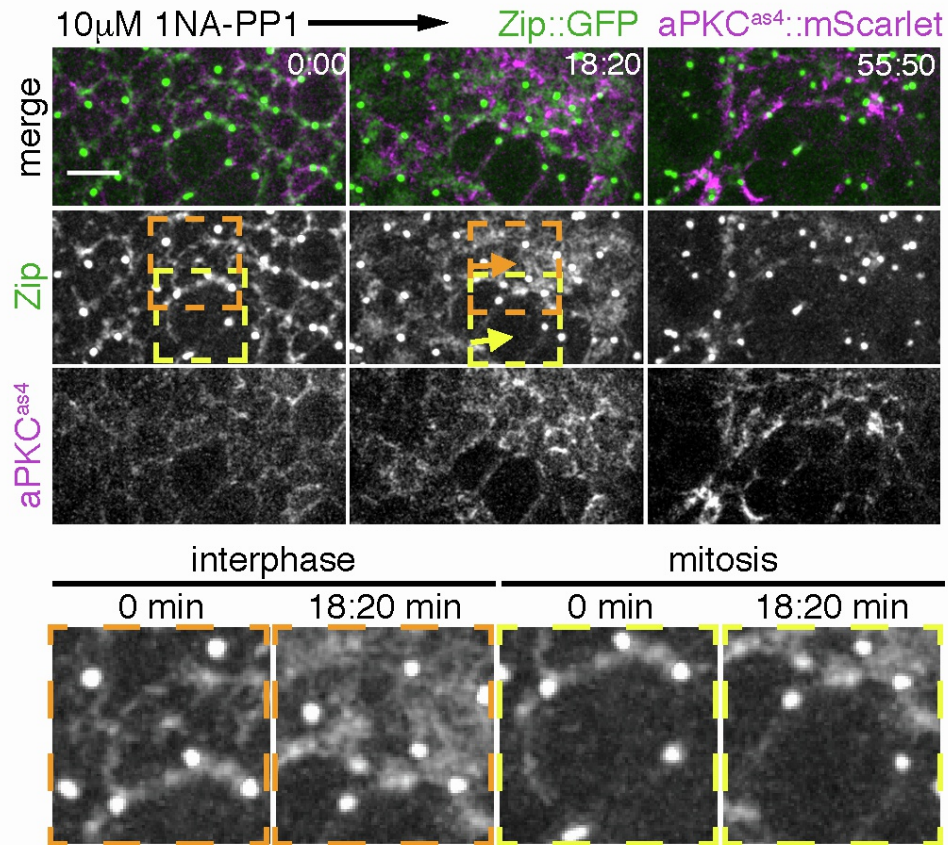


**Figure S4. Myosin enrichment in the apicomedial area upon drug inhibition of aPKC occurs specifically during interphase, Related to Figure 6**

Time-lapse images of *aPKC<sup>as4</sup>::mScarlet* (magenta) and *Zip::YFP* (green) follicle cells treated with 10  $\mu$ M 1NA-PP1 at time 0. Transient apicomedial accumulation of *Zip::YFP* (orange arrow) is not observed in mitotic cells (yellow arrow). Insets show individual interphasic (orange) and mitotic (yellow) cells.

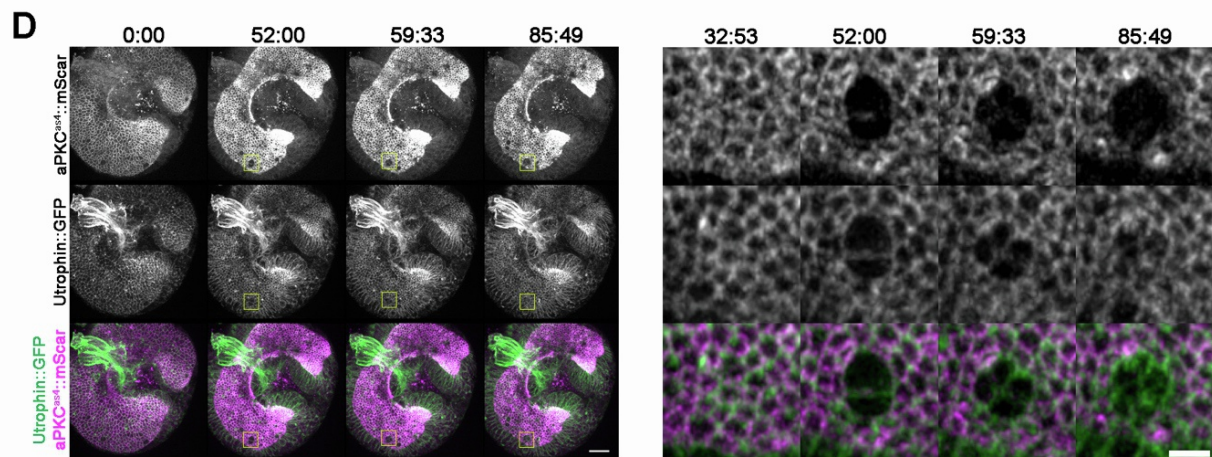
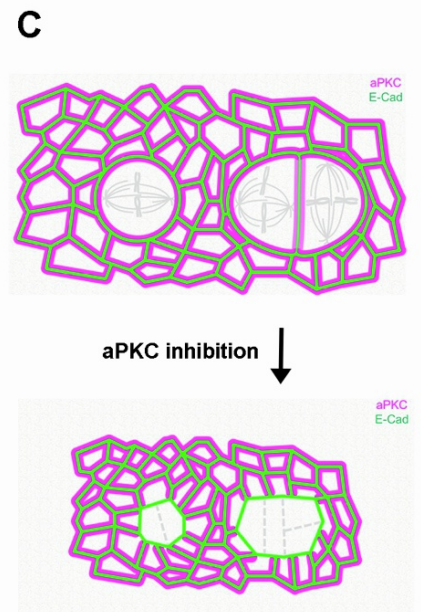
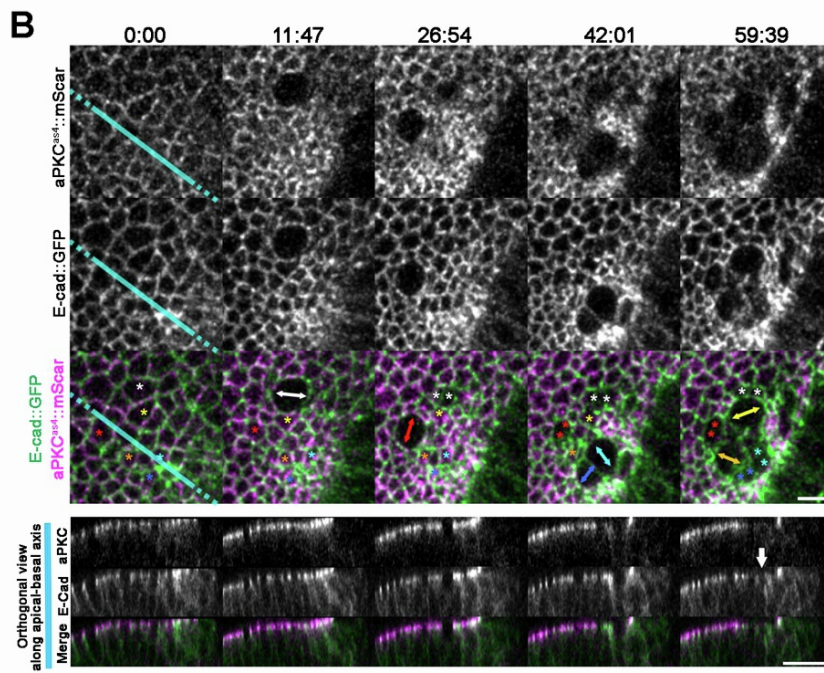
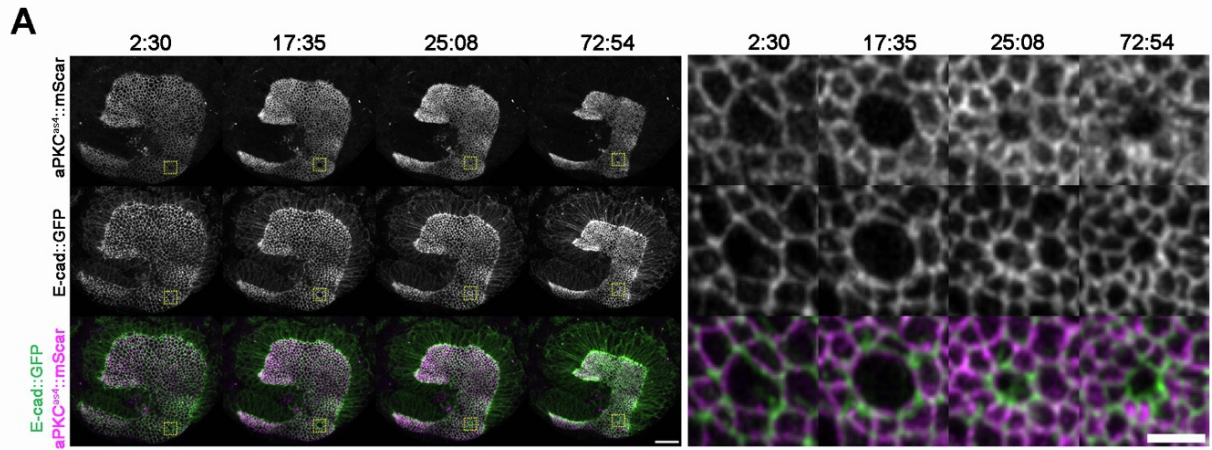




**Figure S5. Acute inhibition of aPKC in the pseudostratified neuroepithelium leads to loss of apical contacts in post-mitotic cells without tissue rupture, Related to Figure 7**

**(A-B)** Time-lapse images of *aPKC<sup>as4</sup>::mScarlet*, E-cad::GFP expressing neuroepithelial tissue upon aPKC inhibition at time 0. **(A)** A close-up (right) of a representative dividing cell shows that the apical contacts of new daughter cells lack aPKC ( $n = 52/62$  cell divisions, 19 larval brains) and E-cad is not enriched at the new daughter-daughter interface ( $n = 16/19$  divisions, 6 larval brains). Scale bars: 20  $\mu\text{m}$  (left) and 5  $\mu\text{m}$  (right). **(B)** Highly proliferative zones can lead to large regions lacking aPKC and E-cad signal at the apical level. The orthogonal view (bottom) shows that this does not correspond to tissue rupture since the post-mitotic unpolarized cells (white arrow) are still present in-between the polarized tissue. Double arrows: orientation of dividing cells. Asterisks: cells before and after the division marked by double arrows of the corresponding colors. Cyan line: location of the orthogonal re-slice shown in the bottom panel. Scale bars: 5  $\mu\text{m}$  (top) and 10  $\mu\text{m}$  (bottom). **(C)** Schematic showing the effect of aPKC inhibition on the localization of aPKC and E-cad in proliferative neuroepithelial cells.

**(D)** Time-lapse images of *aPKC<sup>as4</sup>::mScarlet*, Utrophin::GFP expressing neuroepithelial tissue upon aPKC inhibition at time 0 and the corresponding inset of two adjacent dividing cells (right). Although there is loss of aPKC between all daughter cells ( $n = 8$  pairs of division, 5 larval brains), the post-mitotic cells are still in contact according to the position of their membranes marked with Utrophin::GFP. Scale bar: 5  $\mu\text{m}$ .

Genotype	Optogenetic system activation details
<b>Figure 1</b>	
B ; <i>GFP::aPKC; GR1&gt;Gal4/UAS&gt;LARIAT</i> ; <i>GFP::aPKC/+; GR1&gt;Gal4/UAS&gt;LARIAT</i>	Flies – 2 days
D ; <i>tj&gt;Gal4, GFP::aPKC/GFP::aPKC; (Control)</i> ; <i>tj&gt;Gal4, GFP::aPKC/GFP::aPKC; UAS&gt;LARIAT/+</i> ; <i>tj&gt;Gal4, GFP::aPKC/+; UAS&gt;LARIAT/+</i> ; <i>tj&gt;Gal4, GFP::aPKC/aPKC<sup>k06403</sup>; UAS&gt;LARIAT/+</i>	Flies – 1 day
E ; <i>GFP::aPKC, Lgl::mCherry/GFP::aPKC; UAS&gt;LARIAT/+</i> ; <i>tj&gt;Gal4, GFP::aPKC/GFP::aPKC, Lgl::mCherry; UAS&gt;LARIAT/+</i>	Flies – 1 day
<b>Figure 2</b>	
A ; <i>GFP::aPKC; GR1&gt;Gal4/UAS&gt;LARIAT</i>	Flies – 0, 2, 4, 6 or 12 hours
B,C ; <i>tj&gt;Gal4, GFP::aPKC/GFP::aPKC; UAS&gt;LARIAT/+</i>	Flies – 0, 2, 4, 6 or 12 hours
D ; <i>tj&gt;Gal4, GFP::aPKC/GFP::aPKC; H2A::RFP/UAS&gt;LARIAT</i>	Live imaging
E, F ; <i>aPKC<sup>as4</sup>;</i>	N/A
<b>Figure 3</b>	
A ; <i>tj&gt;Gal4, GFP::aPKC/Lgl::mCherry, GFP::aPKC; UAS&gt;LARIAT/+</i> ; <i>tj&gt;Gal4 GFP::aPKC/GFP::aPKC, E-cad::mKate2x3; UAS&gt;LARIAT/+</i>	Live imaging
B-D ; <i>tj&gt;Gal4, GFP::aPKC/GFP::aPKC; Sqh::mKate2x3/UAS&gt;LARIAT</i>	Live imaging
E,F <i>ubi::nlsRFP, hsFlp, FRT19A/hsFlp, tub&gt;Gal80, FRT19A; tj&gt;Gal4</i> <i>GFP::aPKC/GFP::aPKC, UAS&gt;LARIAT; +</i>  LARIAT expressing cells are marked by bright RFP signal (two nlsRFP copies) and GFP::aPKC clustering.	Live imaging
G, H ; <i>aPKC<sup>as4</sup>::mScarlet;</i>	N/A
I-K ; <i>aPKC<sup>as4</sup>::mScarlet, Zip::YFP/aPKC<sup>as4</sup>::mScarlet</i>	N/A
<b>Figure 4</b>	
A,B ; <i>GFP::aPKC, E-cad::mKate2x3/GFP::aPKC; UAS&gt;LARIAT/+</i> ; <i>tj&gt;Gal4, GFP::aPKC/GFP::aPKC, E-cad::mKate2x3; UAS&gt;LARIAT/+</i>	Live imaging
C,D ; <i>tj&gt;Gal4, GFP::aPKC/GFP::aPKC; +</i> ; <i>tj&gt;Gal4, GFP::aPKC/GFP::aPKC; UAS&gt;LARIAT/+</i>	Ovaries <i>ex vivo</i> – 2 hours
E ; <i>tj&gt;Gal4, GFP::aPKC/GFP::aPKC, UAS&gt;LARIAT; Gal80<sup>ts</sup>/UAS&gt;mCherry</i> ; <i>tj&gt;Gal4, GFP::aPKC/GFP::aPKC, UAS&gt;LARIAT; Gal80<sup>ts</sup> /UAS&gt;Sqh<sup>E20E21</sup></i>	Flies – 2 hours

	<i>; tj&gt;Gal4, GFP::aPKC/GFP::aPKC, UAS&gt;LARIAT; Gal80<sup>ts</sup> /UAS&gt;Sqh<sup>A20A21</sup></i>	
<b>Figure 5</b>		
A	<i>; GFP::aPKC; GR1&gt;Gal4/UAS&gt;LARIAT</i>	Live imaging
B, F-I	<i>; tj&gt;Gal4, GFP::aPKC/GFP::aPKC; H2A::RFP/UAS&gt;LARIAT</i>	Live imaging
C, D	<i>; tj&gt;Gal4 GFP::aPKC/GFP::aPKC; ; tj&gt;Gal4 GFP::aPKC/GFP::aPKC; UAS&gt;LARIAT/+</i>	Ovaries <i>ex vivo</i> – 2 hours
E	<i>; tj&gt;Gal4, GFP::aPKC/GFP::aPKC, UAS&gt;LARIAT; Gal80<sup>ts</sup>/UAS&gt;mCherry ; tj&gt;Gal4, GFP::aPKC/GFP::aPKC, UAS&gt;LARIAT; Gal80<sup>ts</sup>/UAS&gt;Tum RNAi</i>	Flies – 2 hours
<b>Figure 6</b>		
A, B	<i>; tj&gt;Gal4, GFP::aPKC/GFP::aPKC; Sqh::mKate2x3/+</i>	N/A
C	<i>; GFP::aPKC; Sqh::mKate2x3/+</i>	N/A
D-G	<i>; tj&gt;Gal4, GFP::aPKC/GFP::aPKC; Sqh::mKate2x3/+ ; tj&gt;Gal4, GFP::aPKC/GFP::aPKC; Sqh::mKate2x3/UAS&gt;LARIAT</i>	Live imaging
H-I	<i>; GFP::aPKC, E-cad::mKate2x3/GFP::aPKC; UAS&gt;LARIAT/+ ; tj&gt;Gal4, GFP::aPKC/GFP::aPKC, E-cad::mKate2x3; UAS&gt;LARIAT/+</i>	Live imaging
<b>Figure 7</b>		
A, C	<i>ubi::nlsRFP, hsFlp, FRT19A/hsFlp, tub&gt;Gal80, FRT19A; tj&gt;Gal4 GFP::aPKC/GFP::aPKC, UAS&gt;LARIAT; +</i> LARIAT expressing cells are marked by bright RFP signal (two nlsRFP copies) and GFP::aPKC clustering.	Live imaging
B	<i>; tj&gt;Gal4, GFP::aPKC/GFP::aPKC; H2A::RFP/UAS&gt;LARIAT (LARIAT expression in whole tissue) ubi::nlsRFP, hsFlp, FRT19A/hsFlp, tub&gt;Gal80, FRT19A; tj&gt;Gal4 GFP::aPKC/GFP::aPKC, UAS&gt;LARIAT; + (mosaic LARIAT expression)</i>	Live imaging
D	<i>; tj&gt;Gal4/UAS&gt;PatJ::CIBN::pmGFP; UAS&gt;RhoGEF2::CRY2::mCherry/+</i>	Live imaging
E	<i>; tj&gt;Gal4/UAS&gt;PatJ::CIBN::pmGFP; UAS&gt;RhoGEF2::CRY2/Sqh::mKate2x3</i>	Live imaging
F-H	<i>; tj&gt;Gal4/UAS&gt;PatJ::CIBN::pmGFP; UAS&gt;RhoGEF2::CRY2::mCherry/+</i>	Live imaging
I	<i>; tj&gt;Gal4/UAS&gt;PatJ::CIBN::pmGFP; UAS&gt;RhoGEF2::CRY2::mCherry/+</i>	Flies – 2 hours
<b>Supplementary Figure S1</b>		
A	<i>; tj&gt;Gal4, GFP::aPKC/GFP::aPKC; UAS&gt;Par6::mCherry/+ ; tj&gt;Gal4, GFP::aPKC/GFP::aPKC; UAS&gt;Par6::mCherry/UAS&gt;LARIAT ; tj&gt;Gal4, GFP::aPKC/GFP::aPKC; sqh&gt;Cdc42::mCherry /+ ; tj&gt;Gal4, GFP::aPKC/GFP::aPKC; sqh&gt;Cdc42::mCherry/UAS&gt;LARIAT</i>	Flies – 1 day
B	<i>w<sup>1118</sup>;; ; tj&gt;Gal4, GFP::aPKC/GFP::aPKC;</i>	Flies – 1 day



	; <i>tj&gt;Gal4, GFP::aPKC/GFP::aPKC; UAS&gt;LARIAT/+</i> ; <i>tj&gt;Gal4, GFP::aPKC/+; UAS&gt;LARIAT/+</i> ; <i>tj&gt;Gal4, GFP::aPKC/aPKC<sup>K06403</sup>; UAS&gt;LARIAT/+</i>	
C, D	; <i>GFP::aPKC/GFP::aPKC; pnt&gt;GAL4/MKRS</i> ; <i>GFP::aPKC, UAS&gt;LARIAT/GFP::aPKC; pnt&gt;GAL4/MKRS</i>	dark
		Larvae – 1 hour
<b>Supplementary Figure S2</b>		
A	; <i>tj&gt;Gal4, GFP::aPKC/GFP::aPKC; UAS&gt;Par6::mCherry/UAS&gt;LARIAT</i>	Live imaging
B	<i>FRT19A/hsFlp, tub&gt;Gal80, FRT19A; tj&gt;Gal4, GFP::aPKC, E-cad::mKate2/GFP::aPKC, UAS&gt;LARIAT; +</i> LARIAT expressing cells are marked by GFP::aPKC clustering.	Flies 30 min
C-G	<i>ubi::nlsRFP, hsFlp, FRT19A/hsFlp, tub&gt;Gal80, FRT19A; tj&gt;Gal4</i> <i>GFP::aPKC/GFP::aPKC, UAS&gt;LARIAT; +</i> LARIAT expressing cells are marked by bright RFP signal (two nlsRFP copies) and GFP::aPKC clustering.	Ovaries <i>ex vivo</i> – 40 min
H, I	; <i>aPKC<sup>as4</sup> /aPKC<sup>K06403</sup>, E-cad::GFPx3; sqh::mKate2x3/+</i>	N/A
<b>Supplementary Figure S3</b>		
A	; <i>tj&gt;Gal4 GFP::aPKC/GFP::aPKC; Sqh::mKate2x3/UAS&gt;LARIAT</i>	Live imaging
B	; <i>tj&gt;Gal4, GFP::aPKC/GFP::aPKC; UAS&gt;LARIAT/+</i>	Flies – 0, 2 hours
C	; <i>tj&gt;Gal4, GFP::aPKC/GFP::aPKC; UAS&gt;LARIAT/+</i>	ovaries <i>ex vivo</i> , dark
D	; <i>tj&gt;Gal4, E-cad::GFP, Sqh::mKate2x3/+;</i> ; <i>tj&gt;Gal4, E-cad::GFP, Sqh::mKate2x3/+; Gal80<sup>ts</sup>/UAS&gt;Tum RNAi</i>	N/A
E-J	; <i>Ecad::GFP; Sqh::mKate2x3/+</i>	N/A
<b>Supplementary Figure S4</b>		
	; <i>aPKC<sup>as4</sup>::mScarlet, Zip::YFP/aPKC<sup>as4</sup>::mScarlet-I</i>	N/A
<b>Supplementary Figure S5</b>		
A,B	; <i>aPKC<sup>K06403</sup>, E-cad::GFPx3 / aPKC<sup>AS4</sup>::mScarlet-I;</i>	N/A
D	; <i>aPKC<sup>AS4</sup>::mScarlet-I ; Sqh-utrophin::GFP / +</i>	

**Table S1. Genotypes and light exposure details, related to STAR Methods.**

*Drosophila* genotype for each figure panel. When applicable, optogenetic experiment details are indicated: whether optogenetic system was activated by exposing intact flies or dissected ovaries cultured *ex vivo* to blue light and how long samples were exposed to blue light. For live imaging experiments, optogenetic system was only activated after image acquisition started.